

Microscopic Simulation of Limit Cycle Behavior in Spatially Extended Systems

M. Malek Mansour,¹ J. Dethier,¹ and F. Baras¹

Received November 5, 1999; final January 10, 2000

The onset of homogeneous oscillations in spatially extended system is considered. The master equation formulation shows that, in a one-dimensional system, there exists a finite length beyond which the homogeneous oscillations are destroyed. Microscopic simulations are used to investigate the status of this prediction and quantitative agreement is obtained. The origin of the desynchronization mechanism is clarified.

KEY WORDS: Coherent oscillations; microscopic simulations of reactive systems; phase diffusion; Hopf bifurcations; fluctuations.

1. INTRODUCTION

The phenomenological theory of reaction–diffusion systems rests on the fundamental assumption of a clear-cut separation between macroscopic behavior, as described by the equations of chemical kinetics coupled to mass transfer, and the dynamical processes at the microscopic level. Grégoire Nicolis was one of the first scientists to realize that this time-honored hypothesis had to be revised in certain situations.⁽¹⁾ A striking example is provided by transient phenomena involving a long induction period followed suddenly by a violent ignition. On the basis of a probabilistic analysis, Nicolis and his colleagues succeeded in establishing the existence of fluctuation-induced macroscopic effects having no analog in the phenomenological description, such as a considerable dispersion of ignition times and a transient bimodality in the probability distribution.^(2,3) These

¹ Centre for Nonlinear Phenomena and Complex Systems, Université Libre de Bruxelles, Campus Plaine, C.P. 231, B-1050 Brussels, Belgium.

predictions have been shown to apply to a wide range of problems and have been confirmed by experiments in chemistry,⁽⁴⁾ nonlinear optics,⁽⁵⁾ and electronic devices.⁽⁶⁾ In this article we shall be concerned with another puzzling case related to the onset of homogeneous oscillations in spatially extended (unstirred) systems. Started some twenty years ago by Lemarchand and Nicolis,⁽⁷⁾ some intriguing aspects of this problem still remain open.

The time symmetry breaking associated with the transition to a sustained time periodic behavior (Hopf bifurcation) implies some profound changes in the statistical properties of the system. For a homogeneous system, slightly different initial conditions will end up on the deterministic limit cycle with various phases. The macroscopic behavior is thus robust toward fluctuations but phase fluctuations become comparable to the phase itself.⁽⁸⁾ The situation is much more involved in spatially extended systems since the thresholds of successive instabilities are squeezed in a narrow region of parameter space and multiplicity associated to different orientations or phases of the various states accessible to the system is greatly enhanced.⁽⁹⁾ The question then arises as to whether perturbations induced by the microscopic dynamics cannot give rise to a qualitative change by wiping out, through destructive interference, any systematic behavior, thus compromising the very existence of bifurcation.^(10,11)

Recently, one of us (F.B.) studied a 1-dimensional reaction–diffusion system undergoing Hopf bifurcation⁽¹²⁾ through the direct simulation of the associated reaction–diffusion master equation.⁽¹³⁾ The analysis reveals that, as the system size is increased, local fluctuations eventually wipe out the homogeneous oscillation even though the latter is asymptotically stable. The corresponding Langevin formulation have led to the same conclusion.⁽¹⁴⁾ The lack of a proper relaxation mechanism of the phase variable seems to be at the origin of this phenomenon, which marks the limits of validity of the purely macroscopic description of instabilities.⁽¹⁵⁾ This rather surprising conclusion raises naturally the question of the very validity of the stochastic formulation of reactive systems in the presence of Hopf bifurcation. Unfortunately, there exists so far not sufficiently precise experimental data to clarify the situation. In this paper we resort to microscopic simulations to shed some light on this important issue.

The local formulation of the master equation is summarized in the next section, along with a review of the main assumptions underlying this description. Section 3 is devoted to the survey of the microscopic simulation of reactive fluids in the Boltzmann limit. We start our comparative analysis by considering in Section 4 a simple chemical model which allows a detailed discussion of the limit of validity of the reaction–diffusion master equation in the presence of Hopf bifurcation. The main conclusions and perspectives are presented in Section 5.

2. REACTION-DIFFUSION MASTER EQUATION

The basic lines of the master equation formulation of reaction–diffusion systems can be summarized as follows.^(1, 16, 17) We subdivide the reaction volume into spatial cells $\{\Delta V_{\mathbf{r}}\}$ and consider as variables the numbers of particles $\{U_{i\mathbf{r}}\}$ of species $i = 1, 2, \dots$ in these cells. We assume that the set of variables $\{U_{i\mathbf{r}}\}$ defines a Markov process. The random variables $\{U_{i\mathbf{r}}\}$ change as a result of two processes: chemical reactions which will be modeled by a jump Markov process and diffusion whereby a particle may jump to an adjacent cell. The latter will be assimilated to a random walk. The resulting probability distribution $P(\{U_{i\mathbf{r}}\}; t)$ obeys the so-called *multivariate master equation*:

$$\begin{aligned} \frac{d}{dt} P(\{U_{i\mathbf{r}}\}; t) = & \sum_{\mathbf{r}, \{U'_{i\mathbf{r}}\}} W(\{U'_{i\mathbf{r}}\} | \{U_{i\mathbf{r}}\}) P(\{U'_{i\mathbf{r}}\}; t) \\ & + \sum_i \frac{\tilde{D}_i}{2d} \sum_{\mathbf{r}, \ell} \{(U_{i\mathbf{r}} + 1) P(\dots, U_{i\mathbf{r}} + 1, U_{i\mathbf{r}+\ell} - 1, \dots; t) \\ & - U_{i\mathbf{r}} P(U_{i\mathbf{r}}; t)\} \end{aligned} \quad (1)$$

The sum ℓ runs over the first nearest neighbors of the cell \mathbf{r} and \tilde{D}_i is the mean jump frequency of species i . It is related to Fick's diffusion coefficient of the species by:

$$D_i = \frac{\ell_c^2}{2d} \tilde{D}_i \quad (2)$$

where ℓ_c is the characteristic length of a cell and d the space dimension. The explicit form of transition probabilities depends on the reaction scheme and can easily be constructed through combinatorial arguments;⁽¹⁸⁾ they are extensive quantities proportional to the volume $\Delta V = \ell_c^d$ of the cells.

Beside the Markovian hypothesis, the very basics of any stochastic theory of reactive fluids relies on the fundamental assumption that the state of the system can be completely specified in terms of a limited number of macroscopic variables. For isothermal systems, these are just the composition variables. The lumping of all microscopic degrees of freedom except the composition variables can only be justified in systems remaining permanently in a local thermal equilibrium state, which in turn requires a “large” number of molecules per cell. Detailed numerical studies show that a few hundreds of molecules are enough in most practical situations. The local equilibrium assumption is also a necessary condition that allows to approximate the extremely complex motion of molecules by a simple random

walk. We thus conclude that the linear dimensions of a cell should be typically of the order of the reactive mean free path.

The master equation (1) provides an elegant and simple generalization of reaction–diffusion equations. From a theoretical point of view, Nicolis *et al.* have shown that in the close vicinity of a pitchfork bifurcation point its solution can be cast into the exponential of a “stochastic potential,” which turns out to be the Landau Ginzburg potential familiar in equilibrium critical phenomena.^(1, 19) Away from the bifurcation point, it leads to the Langevin reaction–diffusion equations with the correct fluctuation spectrum.^(17–20) In more complex situations, it can easily be studied numerically. Here, the evolution of the system is viewed as a random walk in a discrete phase space (space of “numbers of particles” of different species) for which transitions occur at randomly spaced time intervals. The Markovianity of the process leads to an exponential distribution of waiting times.⁽²¹⁾ From this distribution and the transition probabilities associated to each elementary chemical step, explicit realizations of the process can be constructed, along the lines of a Monte Carlo type of simulation first developed by Gillespie.⁽¹³⁾ Similar techniques are described in ref. 22.

The validity of the master equation (1), however, rests mainly on arguments which, although highly plausible, are nevertheless heuristic and need to be carefully tested. So far, this program has been achieved only in systems where the macroscopic description remains strictly valid.^(23, 24) As we have underline in the Introduction, this seems not to be the case in a 1-dimensional systems undergoing a Hopf bifurcation.

3. MICROSCOPIC SIMULATION OF REACTIVE FLUIDS

The microscopic simulation of reactive fluids involves some basic difficulties that are directly related to the very nature of chemical dynamics. A first problem arises in connection with the validity of the macroscopic rate equations describing the time evolution of the composition variables in dilute (ideal) mixtures. This implies that one needs to have “enough” elastic collisions between consecutive reactive collisions in order to ensure mechanical and thermal equilibrium. As a consequence, only a fraction of the computing time will contribute effectively to the evolution of the system, which results in much wasted bookkeeping with a corresponding waste of CPU time. A second problem is related to the fact that chemical time scales τ_c , like for example the period of a limit cycle in an oscillating system, are frequently in the macroscopic range. To get reliable statistics, one needs to run the corresponding microscopic simulation over a period of time significantly larger than τ_c . This again implies an extremely large amount of running time.

To cope with these difficulties, one is forced to simplify as much as possible both the Newtonian and the chemical dynamics. This can be done by limiting the simulation to hard spheres dynamics and by considering dilute mixtures in the Boltzmann limit for which there exists a powerful algorithm, pioneered by Bird,⁽²⁵⁾ that runs up to three orders of magnitude faster than the corresponding molecular dynamic simulation. Bird's method has become popular since it is in excellent agreement with experimental and molecular dynamic data.^(26, 27) Its basic steps can be summarized as follows.⁽²⁸⁾

As with usual molecular dynamic methods, the state of the system is the set of particle positions and velocities, $\{\mathbf{r}_i, \mathbf{v}_i\}$, $i = 1, \dots, N$ where N is the total number of particles. The evolution is decomposed in time steps Δt , typically a fraction of the mean collision time for a particle. Within a time step, the free flight motion and the particle interactions (collisions) are assumed to be decoupled. The free flight motion for each particle i is computed as $\mathbf{r}_i(t + \Delta t) = \mathbf{r}_i(t) + \mathbf{v}_i(t) \Delta t$, along with the appropriate boundary conditions. After all the particles have been moved, they are sorted into spatial cells, typically a fraction of a mean free path in length. A set of representative collisions, for the time step Δt , is chosen in each cell. For each selected pair a random impact parameter is generated and the collision is performed. After the collision process has been completed in all cells, the particles are moved according to their updated velocities and the procedure is repeated as before. Note that very recently Bird proposed several modifications that improve the performance and the flexibility of his original algorithm.⁽²⁹⁾

We next define what we mean by "reactive hard sphere collisions."^(30, 31) We assign to each species a "color." A reactive collision occurs if the colliding particles have "enough" energy, i.e., if their relative kinetic energy exceeds some threshold related to the activation energy of the reaction. If this is the case, then the colors of the particles are changed, according to the chemical step under consideration. This procedure, however, leads to a continuous energy transfer from reactant to products which induce a deformation of the Maxwell-Boltzmann distribution and can thus modify significantly the values of the rate constants.^(32, 33) To avoid these nonequilibrium effects, the frequency of reactive collisions must be significantly smaller than the frequency of elastic collisions, entailing important waste of CPU time. One way to overcome this difficulty is to further simplify the reactive collision rules by the following procedure. Let us consider a typical bimolecular chemical step:



with

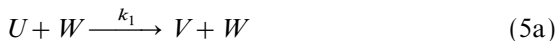
$$k = \nu \exp \left\{ \frac{E}{k_B T} \right\} \equiv \nu k_A \quad (4)$$

where ν is the collision frequency. After a collision between two particles A and B has occurred, we choose randomly $k_A\%$ of the collisions to be reactive, where k_A stands for the Arrhenius factor defined in Eq. (4). Obviously, this procedure avoids the deformation of the Maxwell–Boltzmann distribution, since it does not involve any systematic energy transfer between reactant and products. It is, however, restricted to isothermal chemical systems (see ref. 34 for a review).

It should be noted that such a stochastic treatment of reactive collisions is basically equivalent to the master equation formulation of elementary chemical reactions. In other words, a homogeneous fluctuating reactive Boltzmann equation leads to the very same statistical behavior of composition variables as the corresponding “global” master equation formulation, at least for binary reactions.⁽³⁵⁾ This, however, is not necessarily the case when transport processes are included, since in the Bird algorithm the motion of the particles is handled exactly whereas, in the master equation formulation, reaction and diffusion are viewed as independent elementary processes which in turn allow one to approximate the complex motion of the particles by a simple random walk. In fact, it has been shown on specific examples that the reaction–diffusion master equation is not valid for length scales smaller than the reactive mean free path.⁽³⁶⁾

4. THE MODEL

Simple chemical models exhibiting complex behavior, such as the Brusselator or the Schlögl model, involve trimolecular collisions.⁽¹⁾ The Bird algorithm, however, is restricted to binary collisions only, i.e., to second-order chemical reactions.⁽³⁷⁾ It has been shown that the trimolecular step can be approximated by a pair of bimolecular steps involving different time scales, so that an adiabatic elimination of a fast variable leads to an effective trimolecular step.⁽³⁸⁾ Nevertheless, such a scheme is inappropriate for microscopic simulation because the species represented by the slow variables undergo far fewer reactive collisions per unit time than those represented by fast variables. We thus look here for a chemical model satisfying the following three constraints: (i) it consists of binary collisions only; (ii) it has no significant separation of time scales; (iii) it involves as few reactant as possible. As was shown in ref. 23, the above requirements are fully satisfied by the following chemical model:



where the concentration of S particles (hereafter referred to as “solvent” particles) is supposed to remain constant. This can be achieved by introducing one more participant, say molecules A . Every time an S particle is created (destroyed) in a collision, an $S(A)$ particle is chosen at random in the same collisional cell and replaced by an $A(S)$ particle. Since the A molecules do not participate in any reaction, they merely constitute a reservoir of particles maintaining the solvent concentration fixed. They do, however, modify the microscopic dynamics which, in turn, may interfere with transport processes at the macroscopic level. Extensive molecular dynamic simulations have shown that such an effect, if any, remains negligible, as least for dilute systems.⁽³¹⁾

The reactant are confined in a long thin tube, laterally in contact with a “reservoir” with which it can exchange particles through a semi-permeable membrane. The microscopic realization of such a “feed” process is discussed in ref. 34. The reactor thus operates effectively as a one dimensional open system. Note that laboratory reactors dealing with unstirred systems are quite similar to the one we just described.^(39,40) The macroscopic rate equations corresponding to the model (5) read:

$$\frac{du}{dt} = -k_1 u w + \alpha_u (u_f - u) + D_u \frac{\partial^2}{\partial x^2} u \quad (6a)$$

$$\frac{dv}{dt} = k_1 u - 2(k_2 v^2 - k_{-2} w s) - k_3 v s + \alpha_v (v_f - v) + D_v \frac{\partial^2}{\partial x^2} v \quad (6b)$$

$$\frac{dw}{dt} = k_2 v^2 - k_{-2} w s + D_w \frac{\partial^2}{\partial x^2} w \quad (6c)$$

where u, v, w , and s are the mole fractions of U, V, W and S , respectively; $k_{\pm i}$ are the rate constants of the i th reaction; α_u and α_v are the transfer coefficients (feed rate) of U and V with the reservoir; D_u, D_v and D_w are the diffusion coefficients; and u_f, v_f are the mole fractions of U and V in the reservoir (feed mole fractions), respectively. Periodic boundary condition is adopted and the system is assumed impermeable to W .

The transfer coefficient of a species depends on the diffusion coefficient of that species as well as on the property of the membrane separating the system with the reservoir. For simplicity, in our microscopic simulation we

shall assign to all of the particles same mass and sphere diameter, regardless of their chemical identity. This implies that the diffusion coefficients, and consequently the transfer coefficients, are equal:

$$D_u = D_v = D_w \equiv D \quad (7a)$$

$$\alpha_u = \alpha_v \equiv \alpha \quad (7b)$$

For certain ranges of parameter values, the macroscopic equations (6) can admit multiple steady states and limit-cycle oscillations. In this article we concentrate on a possible occurrence of a Hopf bifurcation. Figure 1 shows the stability diagram for Eqs. (6), where the mole fraction of the V component in the feed stream, v_f , is chosen as the bifurcation parameter, the other parameters being set to:

$$k_1 = k_2 = k_{-2}s = u_f = 1; \quad k_3s = 10\alpha = 0.033 \quad (8)$$

As can be seen, the system undergoes a Hopf bifurcation for a "critical" value v_f^c of the bifurcation parameter located at about $v_f^c \approx 0.2045$. This is confirmed by numerical integration of equations (6) which exhibit sustained oscillations whenever v_f exceeds v_f^c .

For the microscopic simulation, we consider a system made of an assembly of N hard spheres of diameter d confined in a rectangular box of length L with a number density $n = 5 \times 10^{-3}$ particles per d^3 (the mean free path λ is about $45d$). The solvent mole fraction is set to $s = 0.1$, i.e., 10%

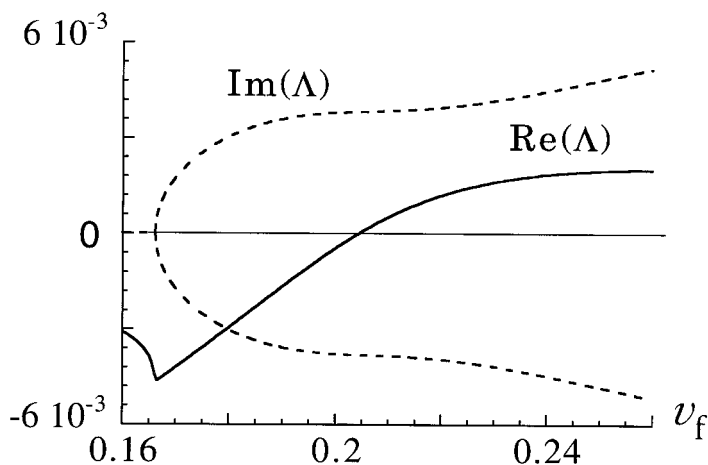


Fig. 1. Bifurcation diagram of the homogeneous macroscopic equations (6). The full line and the dashed line represent the real part and the imaginary part of the largest eigenvalue Λ of the corresponding linearized operator, respectively. The parameters are given in Eq. (8).

of system is made up solvent molecules. All the particles have same mass and diameter, regardless of their chemical (color) identity. For practical convenience, lengths and masses are scaled by the sphere diameter d and the particle mass m , respectively, i.e., we take $d = m = 1$. Similarly, by an appropriate scaling of time and velocities, the temperature and thermal velocity are set to unity. In these units, the Boltzmann constant $k_B = 1/2$, the diffusion coefficient $D = 29.92$ and the collision frequency $\nu = 0.025$. The value of the bifurcation parameter is set to $v_f = 4/15 \approx 0.27$ (recall that of $v_f^c \approx 0.20$). The reactive mean free path is about 4λ which defines the maximum spatial resolution one might expect from the master equation formulation. Accordingly, in our microscopic simulations statistics are taken over spatial cells of precisely 4λ long. Running the program over a single period of oscillations requires about 5000 collisions per particle. A uniform initial state, corresponding to the unstable reference state, is chosen in all reported cases. We start our simulations by setting the average number of particles per cell to about 500, leading to a relatively small noise amplitude of about 5%.⁽⁴²⁾

The space-time plots of Fig. 2 represent the instantaneous result (single run) of such a microscopic simulation for three different cases:

- A "small" system of $L = 32\lambda$ long and containing $N = 4000$ particles.
- An *eight* times longer system ($L = 256\lambda$, $N = 32000$).
- A *forty* times longer system ($L = 1280\lambda$, $N = 160000$).

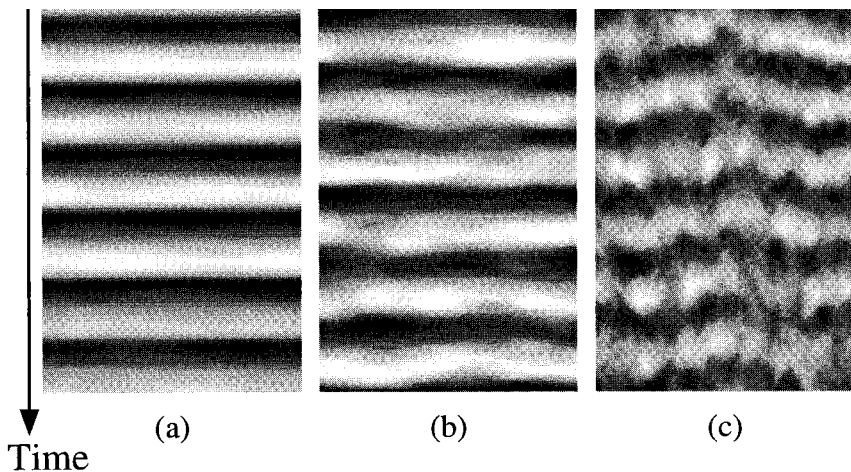


Fig. 2. Space-time plot of the mole fraction of the U species for $L = 32\lambda$ (case (a)), $L = 256\lambda$ (case (b)) and $L = 1280\lambda$ (case (c)). Dark and bright regions indicate high and low mole fractions, respectively. The parameters are given in Eq. (8), with $v_f = 4/15$.

As can be seen, in the case (a) the system oscillates synchronously in a spatially coherent fashion. This same behavior is observed for the case (b), except that now the spatial fluctuations are quite enhanced. The situation is entirely different in the case (c) where different parts of the system oscillate with markedly different phases, picturing a chaotic-like of behavior. The statistical properties of the system follow the above observations. For instance, in case (a) the density of states in phase space remains practically the same as in a 0-d case (crater-like distribution), whereas in case (c) it takes the form of a broad one humped distribution centered on the unstable state.

The simulation of the master equation leads qualitatively to the very same type of behavior. The comparison can be further quantified through the analysis of the space-time auto-correlation function, $C_r(t) = \langle \delta c_r(t) \delta c_0(0) \rangle$, of the fluctuations of a composition variables $\delta c_r(t) \equiv c_r(t) - \langle c_r(t) \rangle$ (note that r is a discrete variable). In order to estimate the statistical errors, we performed a series of 25 runs, each of them consisting of 10^5 collisions per particle, for the microscopic simulations and about 15 times more for the corresponding master equation. In Figs. 3 and 4 we show the real part of the (discrete) spatial Fourier transform, $U_k(t)$, of the correlation function of the U species $\langle \delta u_r(t) \delta u_0(0) \rangle$, for the cases (a) and (b), respectively. Besides the uniform mode ($k=0$), the first non-uniform mode ($k=1$) is also depicted. For each mode, $U_k(t)$ is normalized to unity at $t=0$. This procedure allows to reduce the statistical errors to about 4% for the

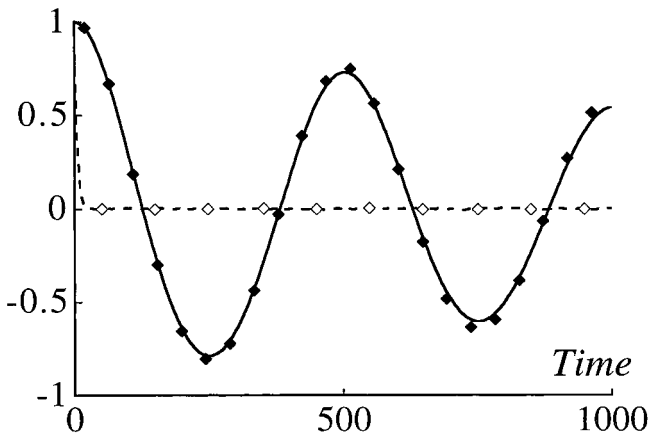


Fig. 3. Normalized time correlation function $\langle \delta u_k(t) \delta u_{-k}(0) \rangle / \langle |\delta u_k|^2 \rangle$ of the U species for $L = 32\lambda$ (case (a)). The full and dashed lines correspond to the homogeneous mode ($k=0$) and to the first inhomogeneous mode ($k=1$), respectively. The diamonds represent the corresponding microscopic results. Parameter values are as in Fig. 2.

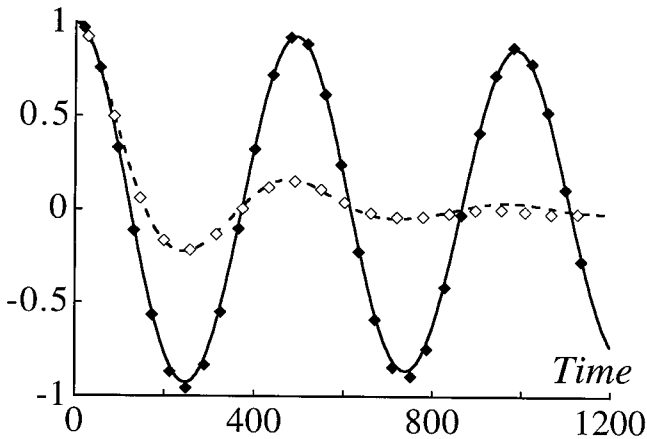


Fig. 4. Normalized time correlation function $\langle \delta u_k(t) \delta u_{-k}(0) \rangle / \langle |\delta u_k|^2 \rangle$ of the U species for $L = 256\lambda$ (case (b)). See caption of Fig. 3 for details.

microscopic simulations and to less than 1% for the master equation simulations. For the case (a), shown in Fig. 3, the inhomogeneous mode vanishes almost instantaneously whereas the homogeneous one shows high persistence, indicating the robustness of the macroscopic limit cycle towards inhomogeneous fluctuations. The same behavior is observed for the case (b), shown in Fig. 4, except that now the inhomogeneous mode shows some persistence extending roughly over two oscillations period. The situation is radically different for the case (c), shown in Fig. 5, where the

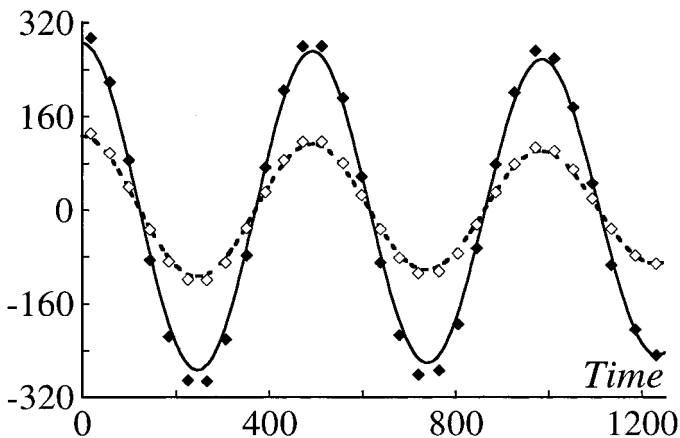


Fig. 5. Time correlation function $\langle \delta u_k(t) \delta u_{-k}(0) \rangle$ of the U species for $L = 1280\lambda$ (case (c)). See caption of Fig. 3 for details.

inhomogeneous mode oscillates very much like the homogeneous one. Furthermore, no significant decay of the correlations is observed in this case, mainly because of the large number of particles involved (small noise). The discrepancy with the master equation results is about 2% for the cases (a) and (b), but grows up to 5% for the case (c), since in this latter case the correlation functions are not normalized to unity at $t=0$.

These results clearly indicate that the time evolution of the system is correctly predicted by the master equation formulation. To complete our analysis, we have also considered a more sensitive test related to the behavior of the static (equal time) spatial correlation function $U_r \equiv \langle \delta u_r(t) \delta u_0(t) \rangle - \delta_{r,0}^{Kr} \langle u \rangle / N_c$, where N_c is the total average number of particles per cell (500 in our case). The results are presented in Fig. 6, together with those obtained from the master equation. Here again, for each case U_r is normalized to unity at $r=0$. The estimated statistical errors remain below 5%, for the first two cases (a) and (b), but become much higher for the case (c), growing up to 20% as r approaches its maximum value, $r/L \approx 0.5$ (recall that the system is periodic).

As can be seen, the decay of the spatial correlation function remains negligible for the case (a) and (b), indicating the highly coherent character of the evolution. On the contrary, in the case (c) the correlation function decays quite rapidly. This loss of spatial coherence is a signature of the destruction of homogeneous oscillatory regime through destructive interferences of local phase fluctuations. In any case, the agreement with the

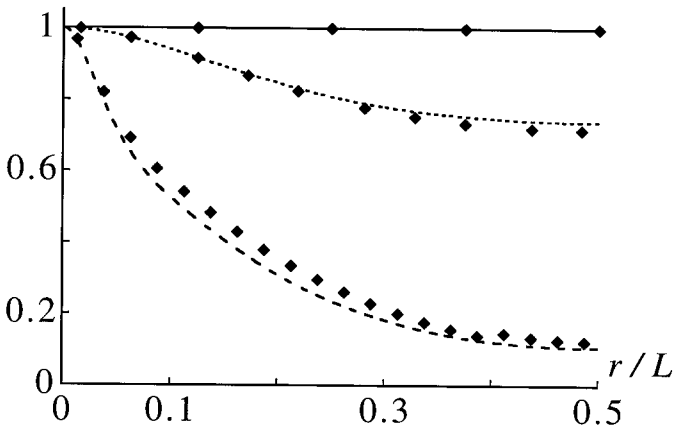


Fig. 6. Normalized static (equal time) spatial correlation function $\langle \delta u(r) \delta u(0) \rangle / \langle (\delta u(0))^2 \rangle$, as a function of r/L . The full line corresponds to $L=32\lambda$ (case (a)), the dotted line to $L=256\lambda$ (case (b)) and the dashed line to $L=1280\lambda$ (case (c)). The diamonds represent the corresponding microscopic results. Parameter values are as in Fig. 2.

master equation prediction is very good, much better than the estimated statistical errors. For instance, the master equation gives 3.33×10^{-3} for the local mole fraction fluctuation $\langle \delta u_r^2 \rangle - \langle u \rangle / N_c$ of the U species, whereas the microscopic simulation leads to about 3.45×10^{-3} , so that the discrepancy remains below 4%.

5. DISCUSSION

In this work microscopic simulations of chemical systems have been used to study the limit of validity of the master equation formulation of reaction–diffusion systems in the presence of Hopf bifurcation. To this end we have introduced a three variable model, particularly well suited for the microscopic simulations. In one dimensional geometry, the results obtained from the associated reaction diffusion master equation indicate that, as the system size is increased, local fluctuations eventually wipe out the homogeneous oscillatory regime, even though the latter is asymptotically stable. Microscopic simulations have confirmed these observations. Detailed analysis of the statistical properties of the system allowed us to establish the validity of the reaction diffusion master equation, including in cases where the corresponding macroscopic description leads to the opposite results.

The above observations raise some fundamental questions, such as the relevance of the dimensionality of the embedding space (affecting the efficiency of the transport mechanism), the effect of the distance from the bifurcation point, the role of the system size (responsible for the multiplicity of unstable modes), etc. Although the complexity of the model precludes any analytical approach, a qualitative analysis remains nevertheless possible.⁽¹⁴⁾

The spatial coherence in reactive systems results from two conflicting processes. On the one hand we have chemical reactions, at the origin of local composition fluctuations and, on the other hand, the mass diffusion which propagates these local fluctuations, giving rise to spatial correlations. The coherence length is thus directly related to the relative importance of the time scales associated to each of these processes. In our case, the slowest reactive time scale is the relaxation time associated to phase diffusion τ_θ . In an homogeneous system, it has been shown by several authors that the phase relaxation time behaves as^(8, 9, 41)

$$\tau_\theta \approx \beta/\varepsilon \quad (9)$$

where β is the distance from the bifurcation point and ε the noise amplitude, inversely proportional to the total number of particles, i.e.,

$$\varepsilon \approx N^{-1} = (nV)^{-1} = n^{-1}L^{-d} \quad (10)$$

During this time, a chemical signal will diffuse over a distance of about $\sqrt{D\tau_\theta}$. The system will therefore remain in a coherent oscillatory state as long as $L \leq \sqrt{D\tau_\theta}$. Taking into account the relation (10), one can write this condition in the form,

$$L^{1-d/2} < \mathcal{C} \sqrt{n\beta D} \quad (11)$$

where \mathcal{C} is a numerical constant, independent of both L and β . Its value cannot be determined within the framework of this simple analysis.

Relation (11) implies a critical dimensionality of 2, in agreement with previous results based on an asymptotic analysis of both master equation⁽⁴³⁾ and stochastic Burgers equation.⁽⁴⁴⁾ Homogeneous oscillations are thus maintained for arbitrarily large three dimensional systems. This is not the case for a one dimensional system where there exists a critical value of L beyond which homogeneous oscillations will always be destroyed. This is precisely what we have observed in our simulations.

The validity of the result (11) can be further investigated through the numerical analysis of two dimensional systems. A microscopic simulation remains beyond the reach of present day computers, since it requires over 2×10^{10} particles, but the master equation simulation still remains tractable. We have considered a two dimensional analogue of the case (c), with a random non uniform initial condition. After an extremely long transient behavior (about two orders of magnitude longer than the corresponding one dimensional case), the system eventually switches to an homogeneous oscillatory regime, in qualitative agreement with predictions of the result (11). Given this prohibitively long CPU time, we were not able to draw any quantitative conclusions. A more promising alternative is the simulation of the associated Langevin equations. Works on this direction is in progress and will be presented elsewhere.

Another puzzling aspect of the problem is related to the asymptotic behavior of the master equation, in the limit $N_c \rightarrow \infty$, N_c being the average total number of particles per cell. As well known, in this limit the probability distribution becomes sharp around the macroscopic path.⁽¹⁹⁾ For large, but finite values of N_c , this property remains true, in the sense that the location of the extrema of the probability distribution still corresponds to the solution of the underlying macroscopic equations (see ref. 34 for a recent review). Now, for the choice of parameters given in Eqs. (13), the macroscopic equations admit a single stationary stable attractor which is a limit cycle (one dimensional manifold). But we have shown that in one dimensional systems there exists a critical system length above which the master equation results always contradict the macroscopic predictions. The question then arises as to the very nature of the chaotic-like of

behavior we have observed in the case (c). Is it intrinsically contained in the macroscopic formulation? If not, how can it be compatible with the fact that the solution of macroscopic equations determines the location of the most probable path of the stochastic process generated by the associated master equation?

One possibility is the existence of stable *time dependent* solutions. In fact, it is well known that the reaction diffusion equations generally admit stable traveling wave solutions,^(45, 46) in addition to a stable limit cycle. These solutions, however, can only exist for a particular class of initial conditions⁽¹⁵⁾ whereas in a stochastic formulation the system can in principle visit the entire phase space (ergodicity). As a consequence, even if we start our stochastic simulation in a traveling wave regime, sooner or later the system will switch to the time periodic regime. This of course does not preclude subsequent random short visits to the traveling wave regime, provided a sufficiently number of unstable modes are excited, i.e., the system is "long enough." This phenomenon gives a plausible explanation of the very origin of the desynchronization mechanism of the homogeneous oscillations. To check the validity of this appealing argument, one has to set up either an analytical or numerical method that allows the construction of the full phase space density by tracing both the stationary time periodic and traveling wave regimes. To our knowledge this problem remains widely open.

ACKNOWLEDGMENTS

We are grateful to Drs. G. Nicolis and J. W. Turner for helpful discussions. This work is supported by the Belgian Federal Office for Scientific, Technical and Cultural Affairs within the framework of the "Pôles d'attractions interuniversitaires" program, and by a European Commission DG 12 Grant PSS*1045.

REFERENCES

1. G. Nicolis and I. Prigogine, *Self-Organization in Nonequilibrium Systems* (Wiley-Interscience, 1977).
2. F. Baras, G. Nicolis, M. Malek Mansour, and J. W. Turner, *J. Stat. Phys.* **32**:1 (1983); G. Nicolis and F. Baras, *J. Stat. Phys.* **48**:1071 (1987).
3. M. Frankowicz and G. Nicolis, *J. Stat. Phys.* **33**:3 (1983); P. Peeters, F. Baras, and G. Nicolis, *J. Chem. Phys.* **93**:7321 (1990).
4. A. Lemarchand, B. I. Ben Am, and G. Nicolis, *Chem. Phys. Letters* **162**:92 (1989); I. Nagypl and I. R. Epstein, *J. Phys. Chem.* **90**:6285 (1986); I. R. Epstein and I. Nagypl, in *Spatial Inhomogeneities and Transient Behaviour in Chemical Kinetics*, P. Gray, G. Nicolis, F. Baras, P. Borckmans, and S. K. Scott, eds. (Manchester Univ. Press, 1990).

5. G. Broggi and L. A. Lugiato, *Phil. Trans. R. Soc. Lond. A* **313**:425 (1984).
6. W. Lange, F. Mitschke, R. Deserno, and J. Mlynek, *Phys. Rev. A* **32**:1271 (1985).
7. H. Lemarchand and G. Nicolis, *Physica A* **82**:251 (1976).
8. K. Tomita, T. Ohta, and H. Tomita, *Prog. Theor. Phys.* **52**:1744 (1974); Y. Kuramoto and T. Tsuzuki, *Progr. Theor. Phys.* **52**:1399 (1974); *ibid.* **54**:60 (1975); J. W. Turner, in *Proceedings of the International Conference on Synergetics*, H. Haken, ed. (Springer, Berlin, 1980); H. Lemarchand, *Physica A* **101**:518 (1980).
9. Y. Kuramoto, *Chemical Oscillations, Waves and Turbulence* (Springer, Berlin, 1984).
10. R. Graham and T. Tèl, *Phys. Rev. A* **42**:4661 (1990); R. Graham, in *Synergetics and Dynamical Instabilities*, G. Gaglioti, H. Haken, and L. Lugiato, eds. (North-Holland, 1988).
11. A. Fraikin and H. Lemarchand, *J. Stat. Phys.* **41**:531 (1985).
12. F. Baras, *Phys. Rev. Lett.* **77**:1398 (1996).
13. D. T. Gillespie, *J. Comput. Phys.* **22**:403 (1976); *ibid.*, *J. Chem. Phys.* **81**:2340 (1977).
14. J. Dethier, F. Baras, and M. Malek Mansour, *Eur. Phys. Lett.* **40**:1 (1998).
15. R. Kapral, in *Lectures Notes in Physics*, L. Schimansky-Geier and T. Poeschel, eds. (Springer-Verlag, Berlin, 1997).
16. K. Kitahara, Ph.D. thesis (Université Libre de Bruxelles, 1974).
17. H. Haken, *Z. Physik B* **20**:413 (1975); C. W. Gardiner, K. J. Macneil, D. F. Walls, and I. S. Matheson, *J. Stat. Phys.* **14**:307 (1976).
18. N. G. Van Kampen, *Stochastic Processes in Physics and Chemistry* (North-Holland, Amsterdam, 1983).
19. M. Malek Mansour, C. Van Den Broeck, G. Nicolis, and J. W. Turner, *Ann. Phys. (USA)* **131**:283 (1981).
20. S. Grossman, *J. Chem. Phys.* **65**:2007 (1976); J. Keizer, *J. Chem. Phys.* **67**:1473 (1977).
21. S. Karlin and H. Taylor, *A First Course in Stochastic Processes* (Academic Press, 1975); D. T. Gillespie, *Markov Processes: An Introduction of Physical Scientists* (Academic Press, 1992).
22. J. S. Turner, *J. Phys. Chem.* **81**:237 (1977); P. Hanusse and A. Blanché, *J. Chem. Phys.* **74**:6148 (1981).
23. F. Baras, J. E. Pearson, and M. Malek Mansour, *J. Chem. Phys.* **93**:5747 (1990); F. Baras, M. Malek Mansour, and J. E. Pearson, *J. Chem. Phys.* **105**:8257 (1996).
24. F. Baras and M. Malek Mansour, *Phys. Rev. E* **54**:6139 (1996).
25. G. A. Bird, *Molecular Gas Dynamics* (Clarendon, Oxford, 1976).
26. D. R. Chenoweth and S. Paolucci, *Phys. Fluids* **28**:2365 (1985); G. A. Bird, *Phys. of Fluids* **30**:364 (1987); E. P. Muntz, *Ann. Rev. Mech.* **21**:387 (1989).
27. R. E. Meyer, *Introduction to Mathematical Fluid Mechanics* (Dover Publ., New York, 1971); G. A. Bird, *Phys. Fluids* **13**:1172 (1970); E. Salomons and M. Mareschal, *Phys. Rev. Lett.* **69**:269 (1992); M. Malek Mansour, M. Mareschal, G. Sonnino, and E. Kestemont, in *Microscopic Simulations of Complex Hydrodynamic Phenomena*, M. Mareschal and B. Holian, eds., Nato ASI Series, Vol. 292 (Plenum Press, 1992), p. 87.
28. A. L. Garcia, *Numerical Methods for Physics* (Prentice-Hall Inc., 1994).
29. G. A. Bird, *Molecular Gas Dynamics and the Direct Simulation of Gas Flows* (Clarendon, Oxford, 1994).
30. P. Ortoleva and S. Yip, *J. Chem. Phys.* **65**:2045 (1976).
31. J. Boissonade, *Phys. Lett. A* **74**:285 (1979); J. Boissonade, in *Nonlinear Phenomena in Chemical Dynamics*, C. Vidal and A. Pacault, eds. (Springer-Verlag, Berlin, 1981); J. Boissonade, *Physica A* **113**:607 (1982).
32. I. Prigogine and E. Xhrouet, *Physica* **15**:913 (1949); I. Prigogine and M. Mahieu, *Physica* **16**:51 (1950).

33. F. Baras and M. Malek Mansour, *Phys. Rev. Lett.* **63**:2429 (1989); M. Malek Mansour and F. Baras, *Physica A* **188**:253 (1992).
34. F. Baras and M. Malek Mansour, *Adv. Chem Phys.* **100**:393 (1997).
35. G. Nicolis, *J. Stat Phys.* **6**:195 (1972).
36. F. Baras and M. Malek Mansour, *Phys. Rev. E* **54**:6139 (1996).
37. A microscopic simulation "mimicking" three-body collisions has been considered successfully by M. Mareschal and A. De Wit, *J. Chem. Phys.* **96**:2000 (1992).
38. S. K. Scott, *Chemical Chaos* (Oxford Science Publ., 1993).
39. V. Castel, E. Dulos, J. Boissonade, and P. De Kepper, *Phys. Rev. Lett.* **64**:2953 (1990); Q. Ouyang and H. L. Swinney, *Nature (London)* **352**:610 (1991).
40. R. Kapral and K. Showalter, eds., *Chemical Waves and Patterns* (Kluwer Academic Publishers, Amsterdam, 1994).
41. F. Baras, in *Lectures Notes in Physics*, L. Schimansky-Geier and T. Poeschel, eds. (Springer-Verlag, Berlin, 1997).
42. C. W. Gardiner, K. J. Mcneil, and D. F. Walls, *Phys. Lett. A* **53**:205 (1975).
43. A. Lemarchand, H. Lemarchand, and E. Sulpice, *J. Stat. Phys.* **53**:613 (1988).
44. D. Walgraef, G. Dewel, and P. Borckmans, *J. Chem. Phys.* **78**:3043 (1983).
45. A. Weber, L. Kramer, I. S. Aranson, and L. Aranson, *Physica D* **61**:279 (1992).
46. G. Nicolis, *Introduction to Nonlinear Science* (Cambridge University Press, 1995).